Macromolecules
ARTICLE

Macromolecules **2009**, *42*, 8889–8898 **8889**
DOI: 10.1021/ma9017179

Extraction of Segment Orientation Distributions in Polymer Networks by Inversion of ^{2}H NMR Spectra through the Maximum-Entropy Method

Bernardo M. Aguilera-Mercado, Claude Cohen, and Fernando A. Escobedo*

School of Chemical and Biomolecular Engineering, Cornell University, Ithaca, New York 14853

Received August 1, 2009; Revised Manuscript Received September 28, 2009

ABSTRACT: We present a simple and computationally inexpensive strategy, to first estimate the average segment-orientation order parameter and then, based on the maximum-entropy method, extract distributions of this order parameter from the conventionally measured ^{2}H NMR spectra. The proposed methodology allows for a more complete characterization of the segmental orientation behavior as compared to solely measuring the observed quadrupolar splittings. The latter approach only quantifies the segment orientation due to local excluded volume interactions, and does not account for the orientation arising from the network topology that is manifested through the width of the spectral "wings". The application of the proposed strategy can be especially advantageous in polymer networks exhibiting highly heterogeneous segment-orientation responses (e.g., bimodal networks) and complex ^{2}H NMR spectrum lineshapes. The methodology is validated with both molecular simulation and experimental results as well as applied to complex spectral data of a PDMS sample.

I. Introduction

Elastomer networks are materials with a great variety of applications; typical examples are O-rings, tires, and rubber bands. These materials can be deformed repeatedly to large extents without losing their properties.[1] These outstanding macroscopic properties are entropic in nature and have their origin in the network structure at the nanoscale.[1,2] For about three decades deuterium nuclear magnetic resonance (^{2}H NMR) experiments have been extensively used in polymer melts and gels to probe microscopic information about configurational entropy, segmental order, and dynamics of polymer chains.[3,4] Such microscopic characterizations have provided valuable experimental evidence to validate various theories in the field of polymer physics.

Most of the ^{2}H NMR experimental studies[5−15] on segmental orientation in strained polymer melts and gels have, however, centered solely on the observed quadrupolar splitting—or doublet—between the peaks of the ^{2}H NMR spectrum. The doublet separation is related to the frequency value that maximizes its distribution (i.e., the most probable value) rather than the average frequency splitting or segment-orientation order parameter.[16−18] The observed splitting is therefore not a measure of the total average orientation of the chain segments but the orientation arising from mean-field-like excluded-volume interactions among the chain segments.[16,19−21] Conversely, the line shape of the NMR spectrum at higher frequencies captures the contribution to segment orientation due to topological network constraints, such as cross-links, and trapped entanglements.[19,22] For instance, networks having a significant fraction of highly stretched end-linked chains—with their chain ends attached to rather distant cross-links—yield NMR spectra with wider "wings".[22]

The total average orientation order parameter (or average frequency splitting) must reflect contributions to segment orientation from both excluded-volume and topological constraints. Hence, the observed splitting of the NMR spectrum may not always be an adequate way to characterize segmental order in elastomeric systems. For example, in some bimodal networks, upon uniaxial deformation, short-chain segments exhibit a significantly higher overall degree of orientation than that of the long-chain segments;[23,24] however, the observed splittings for segments of both short and long chains are very similar.[15] It is relevant to mention that obtaining the average orientation from spectral data is not a trivial calculation. Since the ^{2}H NMR spectrum is the symmetric part of the orientation order parameter distribution,[16] extracting this distribution or its overall average from the spectrum, without any additional information about the shape of the distribution, is an ill-posed problem.

Jacobi et al.[18] estimated the overall average of the order parameter of segmental orientation from the ^{2}H NMR spectrum through products between the arithmetic and harmonic mean-averages of square roots of shifted order parameter absolute values. Such estimation notably overpredicted the overall average order parameter at small uniaxial deformations; as a result, only differences with respect to the unstrained state of the estimated order parameters were considered in that study.[18] Because of the difficulty in estimating the average of the orientation order parameter, measures of the total orientation and its different contributions have been usually obtained from fitting ^{2}H NMR spectral data to multiparameter analytical functions, typically derived from mean-field-based models that involve ideal chain statistics.[19] Nevertheless, mean-field models may not be suitable for an accurate description of systems with highly heterogeneous segmental orientation responses, such as multimodal networks.

Another interesting system in which fitting spectral data to simple mean-field-based models may not be appropriate—particularly due to its ^{2}H NMR spectrum line shape complexities—has been recently documented. In that investigation Genesky and coworkers[25] found a clear (peculiar) shoulder in the ^{2}H NMR spectrum line shape at high extension ratios and two characteristic quadrupolar splittings (two pairs of doublets) on uniaxially stretched and nearly ideal polydimethylsiloxane (PDMS) end-linked networks made of chains with relatively high molar mass.

*Corresponding author. E-mail: fe13@cornell.edu.

Published on Web 10/09/2009

Using a different spectroscopic technique (proton−proton multiple quantum nuclear magnetic resonance) and data analysis approach, Saalwächter et al.[23,26−28] and Gjersing et al.[29] obtained overall averages and distributions of the orientation order parameter on (dry or swollen) unimodal, bimodal, and filled trimodal polymer networks. The authors of those works extracted the distributions of the order parameter from double-quantum build-up intensity curves by numerical Tikhonov regularization[30,31] analysis. The Tikhonov regularization estimates a solution for ill-posed problems involving Fredholm integral equations.[30,31] This regularization approach has also been used to determine order parameter distributions from NMR spectroscopic data in many other systems, such as liquid crystals,[32,33] lipid bilayers,[34] spider dragline silk,[35] and glassy polymers.[36]

Another very well-known and commonly used method for the solution of ill-posed problems is the maximum-entropy method (MEM),[30] which through the maximum-entropy principle yields the least biased and most probable solution estimate based on the given information.[37−39] MEM has been successfully applied to a great variety of systems and experimental techniques to determine, for instance, polystyrene distributions of relaxation times using light scattering,[40] second and fourth orientation order parameters using optical spectroscopy,[41] and structural conformations of organic and biological molecules using ^{1}H NMR and ^{2}H NMR.[42−44] In addition, hybrid schemes using MEM as a complement of the Tikhonov regularization have been recently proposed in order to suppress oscillatory responses, with unphysical negative portions, that the Tikhonov regularization may exhibit in the presence of finite noise.[45] Thus, MEM may as well be an appropriate method choice for interpreting ^{2}H NMR spectral data and obtaining an estimate of the distribution of the orientation order parameter in elastomers.

Herein we present a simple and computationally inexpensive strategy, based on MEM, to extract distributions of the segmental orientation order parameter from the conventionally measured ^{2}H NMR spectra. This proposed methodology allows for a rather accurate description of the segmental orientation behavior in polymer networks as it takes into account the contributions to segment orientation arising from both the so-called excluded-volume effects[16−22] and topological constraints. In addition, the advocated procedure is expected to be especially useful when applied to polymer networks exhibiting highly heterogeneous segmental orientation responses and complex ^{2}H NMR spectrum lineshapes. The rest of this work is organized as follows: first, in section II, we present a derivation of an expression that estimates the overall average frequency splitting or average segment-orientation order parameter in terms of the average absolute value of the order parameter, which can be directly obtained from the ^{2}H NMR spectrum. Also in section II, we use MEM to find the probability distribution of the segment-orientation order parameter from ^{2}H NMR spectrum and the estimated average order parameter. In section III we describe the computational methods and simulated (unimodal and bimodal) networks used to validate the proposed strategy. In section IV we show the results of the validation with spectral data of the simulated networks and experimental PDMS samples, provided by Genesky et al.,[25,46] as well as an application of the proposed methodology to an experimental network with complex spectrum line shape.[25] Finally, we conclude with section V.

II. Theoretical Calculations

II.A. Basic ^{2}H NMR Concepts. Here we recall elementary results of ^{2}H NMR that are relevant for our purpose only; detailed descriptions about the theory of ^{2}H NMR are beyond the scope of this paper and can be found elsewhere.[8,47,48]

If chain segments are in "the fast motion limit", i.e., polymer networks at temperatures above their corresponding glass transition temperatures, the ^{2}H NMR frequency spectrum of a deuterated sample is the result of the superposition of discrete frequency doublets, with separation $|\delta\nu_i|$, from all deuterium-labeled molecules in the system. Each doublet or quadrupolar splitting consists of two delta functions at $\nu = \pm|\delta\nu_i|/2$. The quadrupolar splitting of the ith deuterated unit and its orientation with respect to the applied magnetic field are related by[5]

$$\delta\nu_i = 3/2\delta_Q P_2(\cos\theta_i)^* \quad (1)$$

where δ_Q is the static quadrupolar constant, the P_2 term is the second Legendre polynomial, and θ_i is the angle between the magnetic field and the ith C−^{2}H bond. The asterisk denotes time average over fast segmental reorientations. By taking the average over all of the deuterated units in a uniaxially deformed sample and using the spherical harmonic addition theorem, the overall (or ensemble) average frequency splitting is the following,

$$|\langle\delta\nu\rangle| = 3/2\delta_Q|P_2(\cos\Omega)\langle P_2(\cos\phi_i)^*\rangle\langle P_2(\cos\psi_i)^*\rangle| \quad (2)$$

where angular brackets represent average over all of the deuterated units, Ω is the angle between the magnetic field applied and the strain axis, ϕ_i is the angle between the ith C−^{2}H bond and the vector of the chain-segment to which is attached, and ψ_i is the angle between the ith chain-segment vector and the strain axis. The average segment-orientation order parameter $\langle S^*\rangle$ is $\langle P_2(\cos\psi_i)^*\rangle$. As long as both $P_2(\cos\Omega)$ and $\langle P_2(\cos\phi_i)^*\rangle$ are different from zero, ω can be defined as a dimensionless frequency such that the magnitude of the average dimensionless frequency $|\langle\omega\rangle|$ (i.e., $|\langle\delta\omega\rangle|/2$, which is half of the average dimensionless splitting) is equal to $|\langle S^*\rangle|$. Then, ω is written as:

$$\omega = \frac{\nu}{3/4\delta_Q P_2(\cos\Omega)\langle P_2(\cos\phi_i)^*\rangle} \quad (3)$$

If the total width of the frequency spectrum is large enough when compared to the inverse of the characteristic relaxation time, i.e., where the segments are in "fast motion limit", the spectrum $F(\omega)$ can be written as the symmetrized time-averaged-segment-orientation order parameter distribution,[16] that is

$$F(\omega)\propto\rho(\omega)+\rho(-\omega) \quad (4)$$

where $\rho(\omega)$ (or $\rho(S^*)$) is the probability density distribution of the measured dimensionless frequency or the time-averaged orientation order parameter for the entire population of segments. It is important to emphasize that this distribution $\rho(S^*)$ of the time-averaged orientation order parameter is, by definition, different from the distribution $p(S)$ of the instantaneous orientation order parameter. This is because $\rho(S^*)$ is the resulting distribution from sampling preaveraged values of the order parameter S, which is distributed through the density function $p(S)$. However, the ensemble averages or first moments of these two density distributions are then identical as these functions characterize (under different sampling schemes) the same segment population. Nonetheless, both distributions would be nearly identical in the case of a frozen sample network, wherein all the segments were approximately fixed in space within the duration time of the ^{2}H NMR measurement. The distribution $p(S)$ of the instantaneous orientation order parameter is therefore closely related to the solid state NMR spectrum of

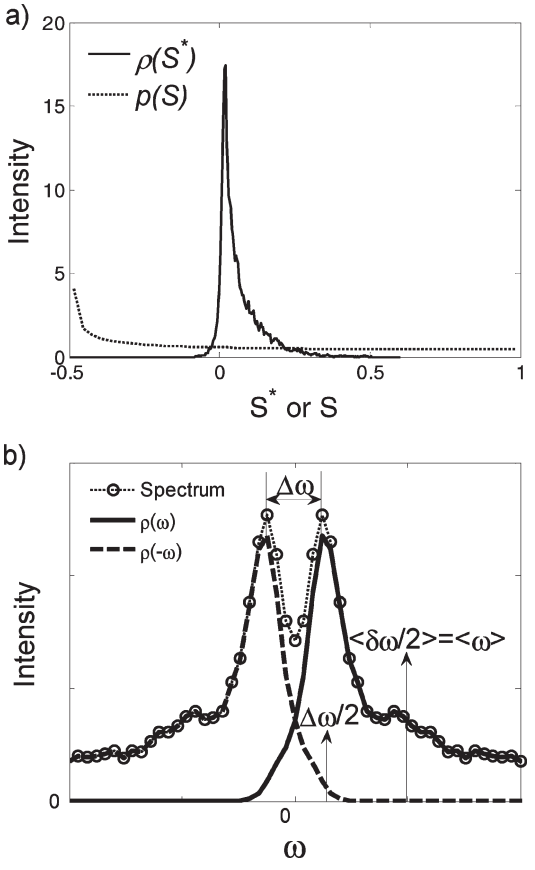

Figure 1. Segment orientation order parameter distributions, frequency spectrum, observed and average frequency splittings. (a) Comparison between the instantaneous and time-averaged orientation order parameter distributions for a simulated unimodal-15-bead network when uniaxially stretched 2.15 times its original size ($\langle S\rangle = 0.06$). (b) Sketch of the relationships between the spectrum, the frequency or order parameter distribution, the observed quadrupolar splitting $\Delta\omega$, the average splitting $\langle\delta\omega\rangle$, and average frequency $\langle\omega\rangle$.

the frozen sample. The qualitative differences in the line shape of these two different distributions of the same population of segments are exemplified in Figure 1a. Further on this article, we focus on the time-averaged orientation order parameter distribution, which is the only one that can be related to ^{2}H NMR measurements in amorphous polymer networks (above their glass transition temperature), and simply refer to it as the orientation order parameter distribution.

The observed frequency splitting $\Delta\omega$, which is twice the magnitude of the most probable frequency $|\omega_{max}|$ (where ω_{max} maximizes $\rho(\omega)$), accounts only for the orientation due to the excluded-volume interactions among the chain segments.[16,19−21] On the other hand, the average frequency splitting $|\langle\delta\omega\rangle|$, twice the magnitude of the average frequency $|\langle\omega\rangle|$, gives a measure of the total degree of orientation, including the orientation contributions from both excluded-volume interactions and topological constraints. A typical sketch, obtained from one of the simulated networks, of the relationships between $F(\omega)$, $\rho(\omega)$, $\Delta\omega$, $\langle\omega\rangle$, and $\langle\delta\omega\rangle$ is shown in Figure 1b.

II.B. Estimating the Average Segment-Orientation Order Parameter. As stated above, the average order parameter $\langle S^*\rangle$ or frequency $\langle\omega\rangle$ cannot be calculated directly from the symmetric function $F(\omega)$, whose odd moments are all equal to zero. However, the average absolute value of the frequency $\langle|\omega|\rangle$ can be obtained from the spectrum $F(\omega)$ in a straightforward fashion as follows:

$$\langle|\omega|\rangle = \int_{-1}^{+1} |\omega|\rho(\omega)d\omega = \frac{\int_{-1}^{+1} |\omega|F(\omega)\,\mathrm{d}\omega}{\int_{-1}^{+1} F(\omega)\,\mathrm{d}\omega} \tag{5}$$

Let $\mathscr{R}$ be defined as the difference between the average absolute value of the frequency and the magnitude of its average. $\mathscr{R}$ can then be written in terms of $\rho(\omega)$ as

$$\mathscr{R} = \langle|\omega|\rangle - |\langle\omega\rangle| = \begin{cases} 2\int_{-1}^{0}(-\omega)\rho(\omega)\,\mathrm{d}\omega & \text{if}\langle\omega\rangle \geq 0 \\ 2\int_{0}^{+1}\omega\rho(\omega)\,\mathrm{d}\omega & \text{if}\langle\omega\rangle < 0 \end{cases} \tag{6}$$

It is important to recall that $\mathscr{R}$ is always greater than or equal to zero, due to the triangle inequality, and for the type of bell-shaped distributions of interest, $\mathscr{R}$ decreases asymptotically toward zero as $|\langle\omega\rangle|$ increases.

Our approach to estimate the average order parameter consists in approximating $\mathscr{R}(|\langle\omega\rangle|)$ through Taylor expansions around the unstretched state when $|\langle\omega\rangle| = |\langle\omega\rangle|_0 = 0$, this is assuming that the sample is isotropic when unstretched. If the segments of the sample were not isotropically distributed at the unstretched state, that is, $|\langle\omega\rangle|_0 > 0$, our approach would then estimate the difference of the order parameter with respect to the unstretched state (i.e., $|\langle\omega\rangle - \langle\omega\rangle_0|$) as only Taylor expansions around that state are performed at this stage. The following step is to assume that $\rho(\omega)$ can be reasonably approximated by translating the distribution at the unstretched state $\rho_0(\omega)$ when $|\langle\omega\rangle - \langle\omega\rangle_0|$ is "small enough", i.e., $\rho(\omega) \cong \rho_0(\omega - \langle\omega\rangle + \langle\omega\rangle_0)$ or simply $\rho(\omega) \cong \rho_0(\omega - \langle\omega\rangle)$ for an isotropic sample. This "translation invariance" approximation is expected to be less accurate when applied to spectral data of relatively short chains (which do not exhibit Gaussian statistics) due to the more pronounced skewness (or asymmetry) of their $\rho(\omega)$ distribution upon deformation; this effect is evidenced by wide spectral "wings" and a severe spectrum broadening upon stretching.

The last step is to perform a Taylor expansion of $\ln(1/\mathscr{R})$ instead of $\mathscr{R}$. Because of this particular choice of expansion, the first term captures the behavior of $\mathscr{R}$ not only at small values of $|\langle\omega\rangle|$ but also at large values of $|\langle\omega\rangle|$ as the resulting approximation for $\mathscr{R}$ decays exponentially to zero with $|\langle\omega\rangle|$. Taylor expanding other functions of $\mathscr{R}$, different from $\ln(1/\mathscr{R})$, can produce similar results as long as their inverses are always positive and decay monotonically to zero. The algebraic details of a slightly more general version of this derivation can be found in the Appendix. Equation 7 is the resulting expression (after neglecting second order terms) from which the magnitude of the average frequency $|\langle\omega\rangle|$ can be estimated. Equation 7 approximately relates $\langle\omega\rangle$ with $|\langle\omega\rangle|$ both scaled with respect to $\langle\omega\rangle_0$, where $\langle|\omega|\rangle_0$ is the average absolute value of the frequency when the sample is unstretched, and gives a measure of the spectrum width.

$$\frac{\langle|\omega|\rangle}{\langle|\omega|\rangle_0} \cong \frac{|\langle\omega\rangle|}{\langle|\omega|\rangle_0} + \exp\left(-\frac{|\langle\omega\rangle|}{\langle|\omega|\rangle_0}\right) \tag{7}$$

It is important to stress that by numerically solving eq 7 an estimate for the magnitude of the average order parameter $|\langle\omega\rangle|$ can be obtained from the average absolute value of the order parameter $\langle|\omega|\rangle$, which can be easily calculated from the ^{2}H NMR spectrum.

This approximation can be extended in order to estimate the magnitude of any odd moment of $\rho(\omega)$ from its symmetric part (or spectrum) $F(\omega)$. Equation 8 results from

generalizing the procedure described above, and allows approximate calculations of magnitudes of higher order odd moments $|\langle\omega^{2k-1}\rangle|$ in terms of average absolute values of odd powers of the order parameter $\langle|\omega|^{2k-1}\rangle$ with $k = 1, 2, ..., M$. These average absolute values of odd powers $\langle|\omega|^{2k-1}\rangle$ can be directly calculated from the spectrum in an analogous way as $\langle|\omega|\rangle$ is obtained from eq 5. Both the derivation of eq 8 and the equivalent version of eq 5 for higher order odd powers can be found in the Appendix.

$$\frac{\langle|\omega|^{2k-1}\rangle}{\langle|\omega|^{2k-1}\rangle_0} \cong \frac{|\langle\omega^{2k-1}\rangle|}{\langle|\omega|^{2k-1}\rangle_0} + \exp\left(-\frac{|\langle\omega^{2k-1}\rangle|}{\langle|\omega|^{2k-1}\rangle_0}\right) \tag{8}$$

II.C. Obtaining the Segment-Orientation Order Parameter Distribution. The probability distribution of the segment-orientation order parameter is estimated from the ^{2}H NMR spectral data by applying MEM, which provides the "best" solution estimates for ill-posed problems given the available information.[37] The information known about the solution is specified through a set of constraints, and MEM yields the solution distribution with the greatest Shannon−Jaynes entropy that satisfies the imposed set of constraints. Here, we present a solution for a discretized probability density function, equally spaced in ω, of the orientation order parameter. The Shannon−Jaynes or information entropy, which in this case is a discretized version of the free energy associated with the orientational entropy of the polymer segments,[8] is defined as[37]

$$A(\rho(\omega_1), ..., \rho(\omega_N)) = -\sum_i [\rho(\omega_i) \ln(\rho(\omega_i))] \tag{9}$$

Herein the available information about the order parameter distribution is written as the following set of constraints:

(1) The distribution has to be normalized.

$$\int_{-1}^{+1} \rho(\omega)\, d\omega = 1 \tag{10}$$

(2) The symmetric part of the distribution must be proportional to the ^{2}H NMR spectrum

$$F(\omega_i) = c\cdot[\rho(\omega_i)+\rho(-\omega_i)] \tag{11}$$

where c is a proportionality constant, which will be absorbed in the normalization constant resulting from constraint 1. It is important to stress that this constraint can be simply written as eq 11 only because chain segments are assumed to be in "the fast motion limit", otherwise the Fourier transform of the relaxation function (written in terms of $\rho(\omega_i)$ and the characteristic relaxation time) should be used instead; this would certainly lead to more complicated algebraic expressions, which may require a numerical solution.

(3) And, the average order parameter is approximately calculated from solving eq 7, that is

$$\int_{-1}^{+1} \omega\rho(\omega)\, d\omega \cong \langle\omega\rangle_{eq\,7} \tag{12}$$

In the strict sense eq 7 estimates $|\langle\omega\rangle|$ instead of $\langle\omega\rangle$, but the sign of $\langle\omega\rangle$ is determined by the type of deformation performed. In uniaxial extension the sign of $\langle\omega\rangle$ is positive, whereas in compression it is negative.

Since we are solving for discrete values of the distribution, the integrals must be replaced by their corresponding and approximated discrete forms. The resulting probability distribution that maximizes $A(\rho(\omega_1), ..., \rho(\omega_N))$, subject to the constraints (eqs 10,11, and 12) can be written in terms of the ^{2}H NMR spectrum as follows:

$$\rho(\omega_i) = \left[\int_{-1}^{+1} \frac{F(\omega)\, d\omega}{1+\exp(-\lambda\omega)}\right]^{-1} \left[\frac{F(\omega_i)}{1+\exp(-\lambda\omega_i)}\right] \tag{13}$$

where λ is the Lagrange multiplier associated with constraint 3, and obtained by solving the following nonlinear equation,

$$\int_{-1}^{+1} \frac{(\omega - \langle\omega\rangle_{eq\,7})F(\omega)\, d\omega}{1+\exp(-\lambda\omega)} = 0 \tag{14}$$

Since the average order parameter from eq 7 is an estimate, the distribution error bars associated with the uncertainty in estimating the average order parameter can be evaluated from:

$$\begin{aligned}\varepsilon(\rho(\omega_i)) &= \left|\frac{\partial\rho(\omega_i)}{\partial\lambda}\frac{\partial\lambda}{\partial\langle\omega\rangle}\right|\varepsilon(\langle\omega\rangle) \\ &= \left|\frac{\rho(\omega_i)\omega_i}{1+\exp(\lambda\omega_i)}\left\langle\frac{\omega(\omega-\langle\omega\rangle_{eq\,7})}{1+\exp(\lambda\omega)}\right\rangle^{-1}\right|\varepsilon(\langle\omega\rangle)\end{aligned} \tag{15}$$

where $\varepsilon(\rho(\omega_i))$ and $\varepsilon(\langle\omega\rangle)$ are the uncertainties in determining $\rho(\omega_i)$ and $\langle\omega\rangle$, respectively.

Information about higher odd moments of the distribution can be similarly included when applying MEM. This may be particularly useful in cases where the line shape of the distribution obtained from eq 13 is very susceptible to small variations of the estimated average order parameter, that is, when the error bars are considerably larger in some specific ranges of frequency. It is worth noting that, in general, the inclusion of additional constraints having inherent uncertainties leads to an overall increase of the solution's uncertainty; nevertheless, including information about the third moment of the distribution may improve the solution stability for some systems.

When the values of the first M odd moments of the distribution, which can be estimated through eq 8, are imposed among the constraints, the resulting distribution from MEM can be written as:

$$\rho(\omega_i) = \left[\int_{-1}^{+1} \frac{F(\omega)\, d\omega}{1+\exp\left(-\sum_{k=1}^{M}\lambda_k\omega^{2k-1}\right)}\right]^{-1} \left[\frac{F(\omega_i)}{1+\exp\left(-\sum_{k=1}^{M}\lambda_k\omega_i^{2k-1}\right)}\right] \tag{16}$$

where λ_k is the Lagrange multiplier associated with the constraint related with the kth odd moment. All the M Lagrange multipliers are now obtained by solving the

Table 1. Characteristics of the Simulated set of Unimodal Networks

chain length (no. of beads)	r_x	no. of chains	no. of cross-links	sol cont. (mass%)	elastic cont. (mol %)
15	1.05	1659	871	0.00	94.7
29	1.10	858	472	0.00	95.6
43	1.05	579	304	0.00	96.7
129	1.15	193	111	0.00	97.4

Table 2. Characteristics of the Simulated Set of (15-300-Bead) Bimodal Networks

short chain content(mol %)	r_x	no. of short chains	no. of long chains	no. of cross-links	sol cont. (mass %)	elastic cont. (mol %)
60	1.15	110	73	105	0.07	74.9
80	1.10	268	67	185	0.25	84.2
90	1.05	490	54	286	0.00	87.3
95	1.10	778	41	451	0.00	90.7
98	1.10	1106	21	621	0.07	92.5

following system of M nonlinear equations,

$$\begin{cases} \displaystyle\int_{-1}^{+1} \frac{(\omega - \langle\omega\rangle_{\text{eq 8}})F(\omega)\,\mathrm{d}\omega}{1+\exp\left(-\sum_{k=1}^{M}\lambda_k\omega^{2k-1}\right)} = 0 \\ \vdots \\ \displaystyle\int_{-1}^{+1} \frac{(\omega^{2M-1} - \langle\omega^{2M-1}\rangle_{\text{eq 8}})F(\omega)\,\mathrm{d}\omega}{1+\exp\left(-\sum_{k=1}^{M}\lambda_k\omega^{2k-1}\right)} = 0 \end{cases} \tag{17}$$

Analogously, the distribution error bars associated with the uncertainty in estimating the first M odd moments can be written as follows:

$$\varepsilon(\rho(\omega_i)) = \sqrt{\sum_{j=1}^{M}\left[\left(\sum_{l=1}^{M}\left(\frac{\partial\rho(\omega_i)}{\partial\lambda_l}\frac{\partial\lambda_l}{\partial\langle\omega^{2j-1}\rangle}\right)\right)^2 \varepsilon^2(\langle\omega^{2j-1}\rangle)\right]} \tag{18}$$

where $\varepsilon^2(\langle\omega^{2j-1}\rangle)$ is the square of the uncertainty in determining $\langle\omega^{2j-1}\rangle$. Derivative terms in eq 18 can be evaluated from:

$$\frac{\partial\rho(\omega_i)}{\partial\lambda_l}\frac{\partial\lambda_l}{\partial\langle\omega^{2j-1}\rangle} = \frac{\rho(\omega_i)\omega_i^{2l-1}}{1+\exp\left(\sum_{k=1}^{M}\lambda_k\omega_i^{2k-1}\right)}\left\langle\frac{\omega^{2l-1}(\omega^{2j-1} - \langle\omega^{2j-1}\rangle_{\text{eq 8}})}{1+\exp\left(\sum_{k=1}^{M}\lambda_k\omega^{2k-1}\right)}\right\rangle^{-1} \tag{19}$$

In short, the process to obtain segment-orientation order parameter distributions from the ^{2}H NMR spectra can be summarized as follows:

(i) Estimate the magnitude of the average frequency or order parameter $|\langle\omega\rangle|$ by numerically solving eq 7.
(ii) Calculate the Lagrange multiplier through eq 14.
(iii) Determine the order parameter distribution and its error bars from eqs 13 and 15, respectively.
(iv) If the error bars are considerably larger in some specific ranges of frequency, include information about the third moment of the distribution (or higher moments if necessary) as follows:
  a Estimate the magnitude of the third (or higher) moment $|\langle\omega^3\rangle|$ from eq 8. The signs of $\langle\omega^{2k-1}\rangle$ and $\langle\omega\rangle$ are the same for the distributions of interests.
  b Calculate the set of Lagrange multipliers by numerically and simultaneously solving the system of nonlinear eqs 17.
  c Determine the order parameter distribution and its error bars from eqs 16, 18, and 19.

III. Molecular Simulation Model and Procedures

Coarse-grained Monte Carlo simulations of polymer networks consisting of unimodal and bimodal chain length distributions were performed in order to validate, along with experimental evidence, the proposed strategy for extracting segment-orientation order parameter distributions from the ^{2}H NMR spectra. The molecular model used in this work has been previously shown to represent well PDMS sample networks in terms of mechanical properties and network microstructure.[24] A brief description of the employed simulation procedures for the polymer end-linking reaction and uniaxial deformation is presented in the following subsections. Detailed information about the simulation methods can be found in ref 24 and works cited therein.

III.A. Network End-Linking. Simulations of the end-linking reaction were carried out on a lattice in the framework of the bond fluctuation model (BFM).[49] This coarse-grained scheme allows for a complete and simultaneous analysis of both static and dynamic quantities in polymeric systems.[50] Here, coarse-grained units (i.e., chain monomers and cross-links) are modeled as cubes capable of forming bonds along any of 108 distinct bond vectors. Only excluded-volume interactions and bonding restrictions are taken into account in this model. The fraction of occupied lattice points was set between 0.46−0.47, a value that has been shown to resemble melt-like conditions.[51] Chains and cross-links were first inserted in the simulation box and then relaxed using hop moves that mimic diffusive dynamics.[50]

After the equilibration stage, which typically involved up to 10^6 moves per repeat unit, the end-linking reaction was initiated by allowing bond formation between chain ends and neighboring tetrafunctional cross-links, while the system continued being equilibrated by the hop moves. The reaction was stopped when the percentage of unreacted chain ends was 1% or lower. The ratio of cross-link arms to chain ends, r_x, used for each simulated system was chosen in order to obtain soluble fractions no greater than 0.3 mass %. The fractions of elastic material—chains that are neither single looped nor pendant—were greater than 95 mol % in the unimodal networks and greater than 75 mol % in the bimodal networks. The size of all systems was set to be approximately equal to allow for a consistent comparison of the different simulated networks. Tables 1 and 2 show the main characteristics of the resulting networks.

III.B. Network Uniaxial Deformation. Monte Carlo simulations of network uniaxial extension were performed off-lattice to allow for continuous deformations of the simulation box. Network coordinates obtained from the on-lattice BFM were transformed into the continuous framework preserving the polymer volume fraction and the network structure. Both chain monomers and cross-links were modeled as Lennard-Jones sites with diameter σ_{LJ} and interaction energy ε_{LJ}. In terms of entanglement chain lengths, each Lennard-Jones site is roughly equivalent to 300 g/mol (~4 monomers) of PDMS.[24] A purely repulsive interaction between nonbonded beads was defined through a cut-shifted Lennard-Jones potential with cutoff at $r_{cut} = 2^{1/6}\sigma_{LJ}$, while bond lengths were allowed to fluctuate between $0.8\sigma_{LJ}$ and $1.2\sigma_{LJ}$. Bond crossing was prevented by setting a bead−bead overlap distance ($r_0 = 0.8\sigma_{LJ}$).

Hop (bead translation), flip (bead rotation) and cluster volume (box dimensions change) moves were implemented, in random order, to equilibrate the system in a pseudodynamic manner.[52] All moves were grouped in cycles. One cycle, which roughly mimics one molecular dynamics step, includes a fixed number (typically equal to the total number of sites in the system) of attempted single-site moves (95% hops and 5% flips) and two volume moves.[53,54] The acceptance ratios for hop, flip and cluster volume moves were 0.30, 0.45, and 0.35, respectively. *NPT* Monte Carlo simulations at temperature $T = 2.0$ (in ε_{LJ}/k_B units) and pressure $P = 3.0$ (in k_BT/σ_{LJ}^3 units) were performed in order to initially equilibrate the system at a melt-like density (~0.8 in $1/\sigma_{LJ}^3$ units). After equilibration (~10^6 cycles), uniaxial extension simulations were subsequently carried out in an isostress ensemble. The imposed stress is given by the difference of applied normal stresses $(P_{xx} + P_{yy})/2 - P_{zz}$, where P_{xx}, P_{yy}, and P_{zz} are the applied normal stresses in the x, y, and z directions, respectively. The extension ratio was obtained from the quotient of the box z-length after the stress was imposed to the initial unperturbed box z-length. Systems were considered to be in equilibrium when their simulation box dimensions reached plateau values, which were typically achieved after 10^7 cycles.

III.C. Simulated ^{2}H NMR Spectra and Order Parameter Distributions. As previously mentioned in Section II.A (eq 4), under certain conditions, generally satisfied for ^{2}H NMR measurements in polymeric systems, the ^{2}H NMR spectrum $F(\omega)$ can be written as the symmetrized distribution of the time-averaged order parameter $\rho(\omega)$.[16] The simulated spectrum can therefore be directly calculated from the order parameter distribution obtained from brute force simulations.[16,17,22] After a (simulated) deformed network reached equilibrium, statistics for each chain segment were taken at every 40 cycles during an additional run of approximately 3×10^7 cycles. At the end of this additional run, the time-averaged order parameter (over the entire additional run) or frequency splitting $\delta\omega$ is calculated separately for each chain segment. The frequency spectrum $F(\omega)$ was obtained from normalizing (by area) an occurrence histogram constructed by adding 1 to the bins corresponding to both $+\delta\omega/2$ and $-\delta\omega/2$ for every chain segment in the system; conversely, the distribution or histogram of the order parameter $\rho(\omega)$ was the result of adding 1 only to the bin corresponding to $\delta\omega/2$ for all the segments. The width of the bins ranged between 0.002 and 0.004.

IV. Results and Discussions

IV.A. Validating the Estimate of the Average Order Parameter. Segment-orientation measurements from both brute force simulations and experimental ^{2}H NMR are used to evaluate the performance of eq 7 and 8 in predicting the magnitudes of the first and higher odd moments of the order parameter distribution.

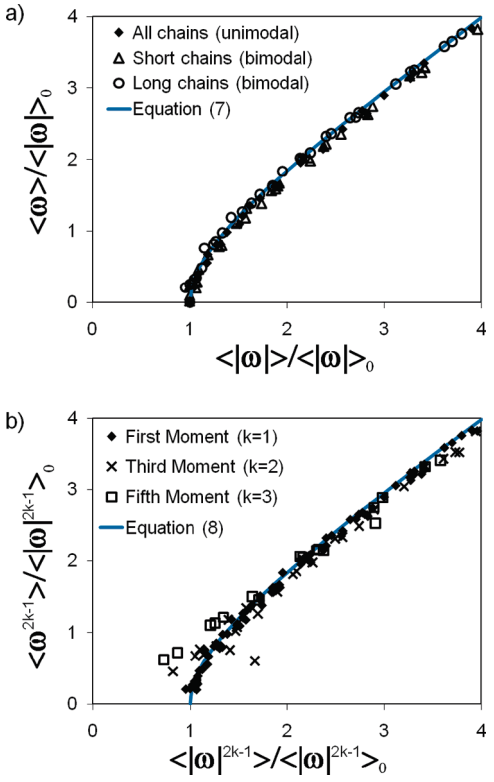

Figure 2. Comparison between predicted (curves) and simulated (symbols) average odd moments for the sets of unimodal and bimodal networks. (a) Scaled average values vs scaled average absolute values of the order parameter distribution. (b) Scaled odd moments vs scaled average absolute odd moments of the order parameter distribution.

A direct comparison between the simulated results and estimations from eq 7 can be made since both the average order parameter and its average absolute value can be calculated in a straightforward manner in simulations. Analogously, direct comparisons can also be made to test the accuracy of eq 8. Figure 2 shows the result of such comparisons. In Figure 2a we can observe that eq 7 predicts rather well the dependence of the (scaled) average order parameter on the (scaled) average absolute value of the order parameter for the simulated results. The mean percentile deviation for all the simulated systems is around 5%. In general, eq 7 tends to slightly overpredict the average order parameter, yet its observed accuracy increases with the length of the polymer chain. For example, in the unimodal networks made with chains of 15, 29, 43, and 129 beads, the mean percentile deviations of eq 7 are 10%, 4%, 2.5%, and 0.5%, respectively. Similarly, for the results of a set of bimodal networks (consisting of chains with 15 and 300 beads) the mean percentile deviations for the short and long chains are 8% and 2%, correspondingly. This accuracy dependence on the chain length is not surprising because longer chains exhibit segment-orientation distributions with less skewness upon deformation (evidenced by a milder spectrum broadening), which favors the applicability of the translation invariance approximation for "small" deformations that was assumed in section II.B. This suggests that for segments of non-Gaussian (or relatively short) chains the difference $\mathscr{R}$ decays with the average at a slower rate than the exponential approximation. From Figure 2b analogous results are

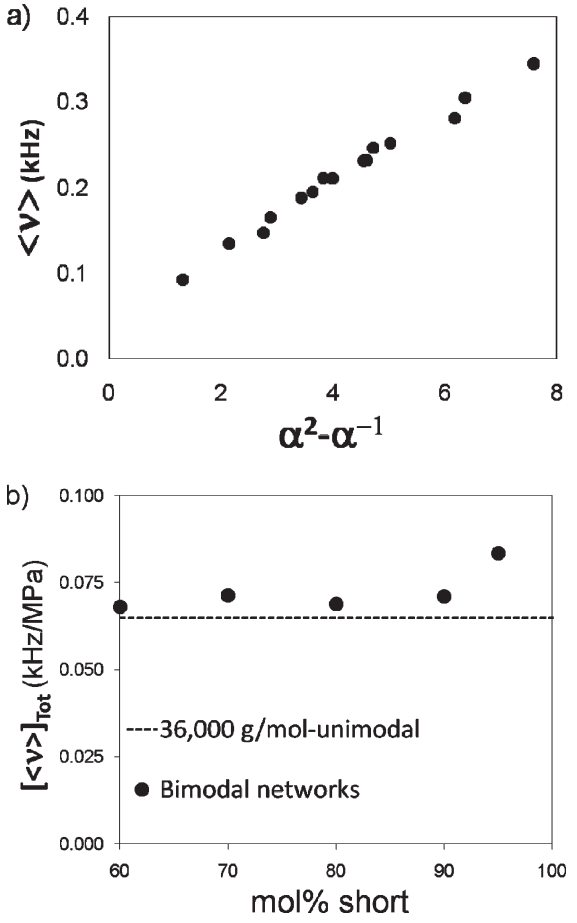

Figure 3. Estimates of the average frequency and the total reduced frequency for PDMS networks. (a) Estimated average frequency (eq 7) vs extension for the 36-kg/mol-unimodal PDMS network. (b) Estimated total reduced frequency for the 36-kg/mol-unimodal PDMS network (dashed line) and several (5.0/4.5−90/80 kg/mol) bimodal PDMS networks with different molar content of short chains (solid circles).

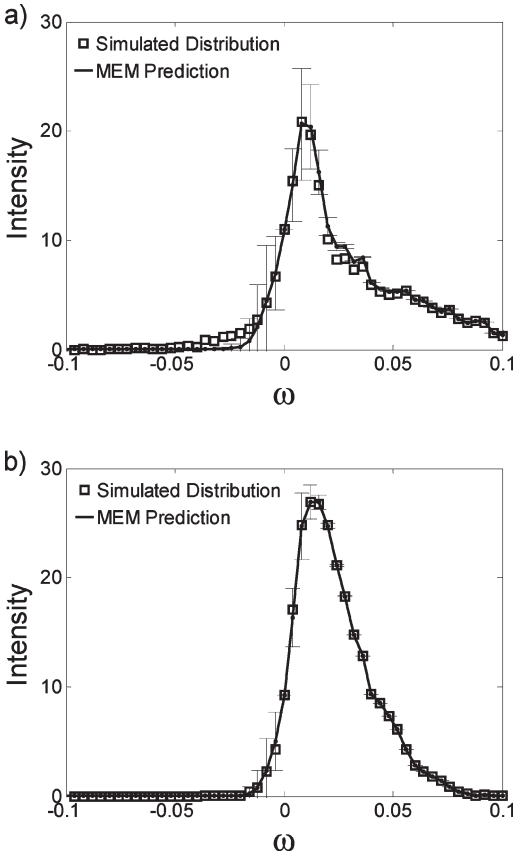

Figure 4. Comparison between order parameter distributions directly obtained from molecular simulations (empty squares) and their corresponding MEM predictions (solid lines) for a simulated bimodal network consisting of 90 mol % of 15-bead chains and 10 mol % of 300-bead chains when $\alpha = 2.15$. Orientation order parameter distributions for (a) the short (15-bead) chains and (b) the long (300-bead) chains.

obtained for the performance of eq 8 when predicting magnitudes of the third and fifth moments of the order parameter distribution. However, when estimating higher odd moments the noise of the frequency spectrum is also amplified, which leads to an additional increase of uncertainty in the estimation of such moments.

Although the predictions of eq 7 cannot be directly compared with experimental results, indirect quantitative comparisons, based on theoretical relations, may be performed to evaluate the quality of the predictions. Specifically, we know from classical theory of rubber elasticity[2,3] and from experimental evidence[15] that the average orientation order parameter is proportional to Young's modulus E and the network deformation term $\alpha^2 - \alpha^{-1}$, where α is the extension ratio. Then, the reduced frequency $[\langle\nu\rangle]$, defined below, is expected to be very similar for polymer networks made of the same chemical monomer.[3]

$$[\langle\nu\rangle] = \frac{\langle\nu\rangle/E}{\alpha^2 - \alpha^{-1}} \tag{20}$$

Figure 3a shows the expected linear dependence of the estimated average frequency $\langle\nu\rangle$ on the extension term $\alpha^2-\alpha^{-1}$ for a nearly unimodal PDMS end-linked network with chains having number-average molar mass of 36 kg/mol.[25] Moreover, Figure 3b depicts the comparison between the predicted values for the total reduced frequencies $[\langle\nu\rangle]$ in several bimodal PMDS networks and the 36-kg/mol-unimodal network. For all bimodal networks, total reduced frequencies are calculated as the mass-weighted averages of the reduced frequencies of short and long chains. Predicted reduced frequencies $[\langle\nu\rangle]$ are rather similar for all the studied networks regardless of the differences in chain polydispersity. All the bimodal networks were the result of end-linking two sets of chains with number-average molar mass of 5.0−4.5 kg/mol and 90−80 kg/mol in different proportions. The synthesis of the different deuterated systems and ^{2}H NMR measurements were performed by Genesky et al.[25,46] From Figure 3 we can infer that the estimates of the average order parameter obtained from eq 7 agree relatively well with the predictions of classical theory of rubber elasticity.

Altogether, these results and those for the direct comparisons with simulated networks suggest that the proposed methodology to estimate the average order parameter (and higher odd moments of the distribution) from spectral data can be used quantitatively within a rather acceptable range of uncertainty (5%−10%).

IV.B. Validating the Estimated Order Parameter Distribution. Here order parameter distributions extracted by interpreting spectral data through MEM are compared with the corresponding distributions obtained from brute force Monte Carlo simulations. The system used for the comparisons is a bimodal network, which exhibits considerably high degree of heterogeneity in its segment-orientation responses of the short and long chains. This bimodal network consists

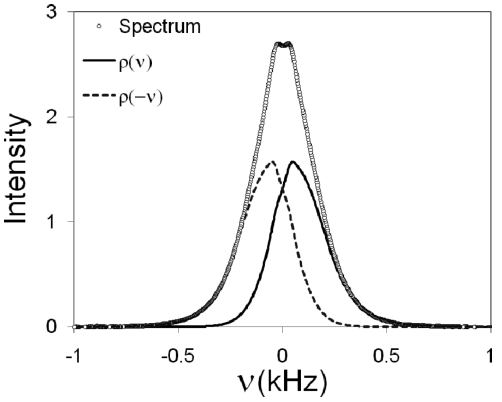

Figure 5. Frequency spectrum (empty circles) and its decomposition into the predicted frequency distribution (solid line) and its mirror image (dashed line), for the 36-kg/mol-unimodal PDMS network when $\alpha = 1.42$.

of 90 mol % of 15-bead (short) chains and 10 mol % of 300-bead (long) chains. More information about this network can be found in Table 2. Figure 4 illustrates good agreement between the distributions obtained from simulations and their estimates calculated through MEM for both short and long chains in the network stretched to $\alpha = 2.15$. Only information about the first moment was used in these comparisons. Error bars are calculated assuming a 5% of uncertainty in the $\langle\omega\rangle$ estimation. As expected from the assumptions made in section II.B, the accuracy of the distribution estimates also increases with chain length.

The observed (dimensionless) frequency splitting for both types of chains in the network is in the order of 2×10^{-2}, whereas the average frequency (or order parameter) for the short and long chains are 5.27×10^{-2} and 2.30×10^{-2}, respectively. For comparison, the estimates from eq 7 of the average order parameters for the short and long chains of this system are 5.5×10^{-2} and 2.3×10^{-2}, and the corresponding predicted values of the average order parameters obtained from fitting spectral data to the mean-field-based Gaussian network model of Ries et al. (eqs 9 and 10 of ref 19) are 12.9×10^{-2} and 1.77×10^{-2}. As the model presented by Ries et al. involves ideal chain statistics, specifically affine deformation, important deviations are expected for the short chains of 14 segments since they exhibit a pronounced non-Gaussian behavior.

Another interesting feature of this bimodal network is that the large difference in the orientation response among the different chains in the network is not captured well by the observed splittings, and is clearly evidenced by the distinct spectra lineshapes. Such a difference in the orientation response between the short and long chain segments is attributed to the fact that short chains are significantly more stretched than their longer counterparts in certain bimodal networks.[23,24] It is important to stress that these types of systems represent a good example of the potential applicability of the advocated methodology to quantitatively characterize the orientational behavior in polymer networks with heterogeneous orientation responses from the conventional ^{2}H NMR measurements.

IV.C. Application to an Experimental PDMS Network. By means of the proposed method, frequency splitting distributions are estimated, from their corresponding ^{2}H NMR spectra, for the 36-kg/mol-unimodal PDMS network[25] at low and high uniaxial deformations. Figure 5 shows the ^{2}H NMR frequency spectrum and the predicted frequency distribution of this unimodal PDMS network at extension ratio

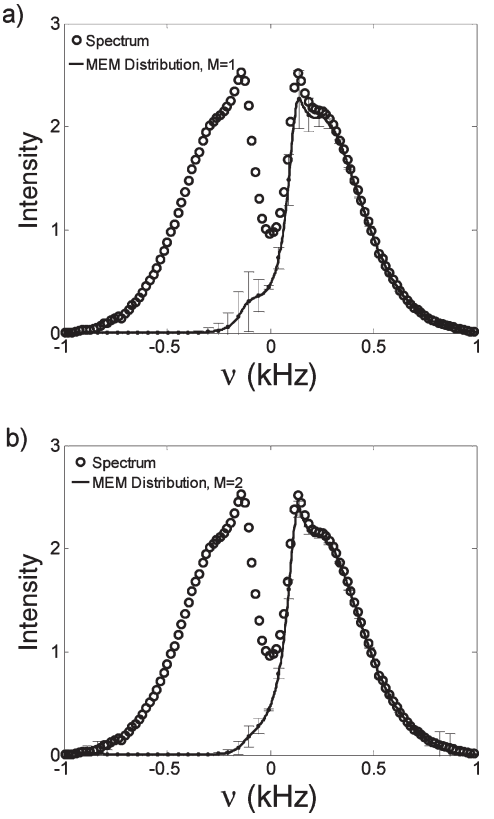

Figure 6. Frequency spectrum (empty circles) and the predicted frequency distributions (solid lines), for the 36-kg/mol-unimodal PDMS network when $\alpha = 2.56$. (a) MEM prediction using information about the first moment only (eq 16 with $M = 1$). (b) MEM prediction using information about the first and third moments (eq 16 with $M = 2$).

$\alpha = 1.42$; only information about the first moment was used. Although the quadrupolar splitting is not clearly visible in the spectrum at such moderate deformation, the observed frequency splitting, in addition to the average splitting, can be determined from the predicted distribution. Interestingly, when this 36-kg/mol-unimodal PDMS network is greatly stretched ($\alpha = 2.56$), its ^{2}H NMR spectrum (Figure 6) shows a clear and unusual shoulder, that is, two characteristic quadrupolar splittings are observed.[25] The existence of these two splittings at high extensions may be attributed to a great disparity in the chain end-to-end distance distribution which could lead to such heterogeneous orientation response within the network. Figure 6a shows the estimated frequency distribution when only information about the first moment or average of the distribution is included. All error bars are calculated assuming a 5% of uncertainty in the $\langle\nu\rangle$ estimation. The solution distribution yielded by MEM for this complex lineshaped-spectrum seems very sensitive to small variations of the estimated average; in order to improve the stability of the solution, information about its third moment was also included in MEM. The result of this second attempt is shown in Figure 6b where a significant improvement in the distribution stability is observed for this complex spectrum; however, if information about the fifth moment is included as well, the resulting error bars in the distribution are much larger and the distribution line shape is less smooth in some frequency ranges (not shown). In this case then, the first and third moments provide the amount of information that optimizes stability of the solution distribution.

As illustrated with this last system, another instance wherein the proposed methodology of estimating segment-orientation distributions may be especially advantageous is

in interpreting ^{2}H NMR spectral data of systems exhibiting complex spectra, which cannot be trivially analyzed through the conventional treatment of multiparameter fitting of spectral data to ideal-chain-like models.

V. Conclusions

An analytical expression was derived, based on suitable Taylor expansions, to estimate the magnitude of the average order parameter and higher odd moments from spectral data (i.e., from average absolute values of the order parameter or average absolute moments). It was found through comparisons with simulated and experimental results that the derived expression can estimate the average order parameter within an acceptable range of uncertainty (5% to 10%), whose accuracy increases for systems showing more completely averaged spectra (e.g., networks consisted of "long" chains). The latter is due to the translation invariance approximation for "small" deformations used in Section II.B when deriving the estimate for the average order parameter.

In principle, the accuracy of the estimation of the average order parameter for networks containing "too short" chains could be improved by using more flexible schemes, but at the expense of losing generality. For example, one could Taylor-expand a different function of $\mathscr{R}$, instead of $\ln(1/\mathscr{R})$, that allows for tuning how fast $\mathscr{R}$ decays with the average. For instance, by choosing $1/\mathscr{R}^h$, the free parameter h would modulate the decay of $\mathscr{R}$; and for a given set of data, the most appropriate value of h could be found such that one observes the expected dependence of the average order parameter $\langle\nu\rangle$ on $\alpha^2-\alpha^{-1}$ (i.e., linear and with very small or null intercept).

On the basis of the maximum-entropy method, an alternative strategy for interpreting the ^{2}H NMR spectral data was developed. This simple and computationally inexpensive strategy, which requires the numerical solution of a few nonlinear equations only, is capable to accurately extract distributions of the segmental orientation order parameter from the conventionally measured ^{2}H NMR spectra. The proposed methodology can be especially advantageous when applied to polymer networks exhibiting highly heterogeneous segmental orientation responses and complex ^{2}H NMR spectrum lineshapes. Such systems may not be appropriately analyzed through the conventional treatments—multiparameter fitting of spectral data to ideal-chain-mean-field-like models or solely measuring the observed quadrupolar splittings.

Acknowledgment. This work was supported by the National Science Foundation Polymers Program under Grant DMR-0705565. We thank T. Michael Duncan and Geoffrey D. Genesky for helpful discussions and providing the critical ^{2}H NMR spectral data of the PDMS networks.

Appendix

AI.A. Derivation of eq 8. The average absolute values of odd powers of the order parameter $\langle|\omega|^{2k-1}\rangle$ (with $k = 1,2, ..., M$) can be calculated from spectral data as follows

$$\langle|\omega|^{2k-1}\rangle = \int_{-1}^{+1} |\omega|^{2k-1}\rho(\omega)\,\mathrm{d}\omega = \frac{\int_{-1}^{+1} |\omega|^{2k-1}F(\omega)d\omega}{\int_{-1}^{+1} F(\omega)\,\mathrm{d}\omega} \quad \text{(A-1)}$$

Let $\mathscr{R}_{2k-1}$ be defined as the difference between $\langle|\omega|^{2k-1}\rangle$ and $|\langle\omega^{2k-1}\rangle|$. Then, $\mathscr{R}_{2k-1}$ can then be written in terms of $\rho(\omega)$ as follows:

$$\mathscr{R}_{2k-1} = \langle|\omega|^{2k-1}\rangle - |\langle\omega^{2k-1}\rangle| = \begin{cases} 2\int_{-1}^{0}(-\omega^{2k-1})\rho(\omega)\,\mathrm{d}\omega & \text{if}\langle\omega^{2k-1}\rangle \geq 0 \\ 2\int_{0}^{+1}\omega^{2k-1}\rho(\omega)\,\mathrm{d}\omega & \text{if}\langle\omega^{2k-1}\rangle < 0 \end{cases} \quad \text{(A-2)}$$

Subsequently, $\ln(1/\mathscr{R}_{2k-1})$ is Taylor expanded around the unperturbed state, $|\langle\omega^{2k-1}\rangle| = |\langle\omega^{2k-1}\rangle|_0$, assuming first that all segments are isotropically distributed when the sample is unstretched (i.e., $|\langle\omega^{2k-1}\rangle|_0 = 0$ and $|\langle\omega\rangle|_0 = 0$), and second that $\rho(\omega)$ can be reasonably approximated by translating the distribution at the unstretched state $\rho_0(\omega)$ when $|\langle\omega\rangle - \langle\omega\rangle_0|$ (or equivalently $|\langle\omega^{2k-1}\rangle - \langle\omega^{2k-1}\rangle_0|$) is "small enough", i.e., $\rho(\omega) \cong \rho_0(\omega - \langle\omega\rangle + \langle\omega\rangle_0)$. After some algebraic manipulations of the aforementioned the Taylor expansion, the following expressions result: If $\langle\omega^{2k-1}\rangle \geq 0$,

$$-\ln\left(\frac{\mathscr{R}_{2k-1}}{\langle|\omega|^{2k-1}\rangle_0}\right) = -\frac{\langle\omega^{2k-1}\rangle}{\langle|\omega|^{2k-1}\rangle_0}\frac{\mathrm{d}\langle\omega\rangle}{\mathrm{d}\langle\omega^{2k-1}\rangle}\bigg|_0 \frac{\mathrm{d}}{\mathrm{d}\langle\omega\rangle}\left(2\int_{-1-\langle\omega\rangle}^{-\langle\omega\rangle} -(\omega+\langle\omega\rangle)^{2k-1}\rho_0(\omega)\,\mathrm{d}\omega\right)\bigg|_0 \quad \text{(A-3a)}$$

And, if $\langle\omega^{2k-1}\rangle < 0$,

$$-\ln\left(\frac{\mathscr{R}_{2k-1}}{\langle|\omega|^{2k-1}\rangle_0}\right) = -\frac{\langle\omega^{2k-1}\rangle}{\langle|\omega|^{2k-1}\rangle_0}\frac{\mathrm{d}\langle\omega\rangle}{\mathrm{d}\langle\omega^{2k-1}\rangle}\bigg|_0 \frac{\mathrm{d}}{\mathrm{d}\langle\omega\rangle}\left(2\int_{-\langle\omega\rangle}^{1-\langle\omega\rangle} (\omega+\langle\omega\rangle)^{2k-1}\rho_0(\omega)\,\mathrm{d}\omega\right)\bigg|_0 \quad \text{(A-3b)}$$

The subscript "0" denotes that the evaluations of the expressions have to be at the unstretched state (that is, when $|\langle\omega\rangle| = 0$ and $|\langle\omega^{2k-1}\rangle| = 0$). The derivatives of the integrals in eq A-3 can be evaluated by the application of the Leibniz integral rule or the Reynolds transport theorem for one dimension; in this step we also assume that $\rho_0(\pm1) = 0$. The resulting derivatives are $\pm(2k-1)\langle-\omega^{2k-2}\rangle_0$ respectively. The derivative of $\langle\omega\rangle$ with respect to $\langle\omega^{2k-1}\rangle$ is obtained from the following binomial expansion

$$\frac{\mathrm{d}\langle(\omega-\langle\omega\rangle)^{2k-1}\rangle}{\mathrm{d}\langle\omega\rangle}\bigg|_0 = \frac{\mathrm{d}}{\mathrm{d}\langle\omega\rangle}\left(\sum_{i=0}^{2k-1}\frac{(2k-1)!}{(i)!(2k-1-i)!}\langle\omega^{2k-1-i}\rangle\langle-\omega\rangle^i\right)\bigg|_0 \quad \text{(A-4a)}$$

After isolating the term involving $\langle\omega^{2k-1}\rangle$ and evaluating at the unperturbed state the polynomial terms, we find

$$\frac{\mathrm{d}\langle\omega\rangle}{\mathrm{d}\langle\omega^{2k-1}\rangle}\bigg|_0 = \left((2k-1)\langle\omega^{2k-2}\rangle_0 + \frac{\mathrm{d}\langle(\omega-\langle\omega\rangle)^{2k-1}\rangle}{\mathrm{d}\langle\omega\rangle}\bigg|_0\right)^{-1} \quad \text{(A-4b)}$$

At this point we invoke our translation invariance approximation, i.e., $\rho(\omega) \cong \rho_0(\omega - \langle\omega\rangle)$, which also implies that all

central moments should not change significantly around $|\langle\omega\rangle|_0 \cong 0$ (as the resulting entire distribution is reasonably well described by just a small translation of the distribution of the reference state); as a result this approximation implies that

$$\left|\frac{d\langle(\omega-\langle\omega\rangle)^{2k-1}\rangle}{d\langle\omega\rangle}\right|_0 \ll (2k-1)\langle\omega^{2k-2}\rangle_0 \qquad \text{(A-5)}$$

Equation A-5 explains the statement on section II.B about the dependence of the accuracy of the translation invariance approximation on the skewness (or asymmetry) of the distribution upon deformation. Spectral data from networks containing relatively short chains are more likely to poorly satisfy eq A-5, as severe spectrum broadening upon sample deformation is a manifestation of considerable changes of the central odd moments.

The next step is to substitute eqs A-5, A-4b, and the resulting of derivatives of the integrals into eqs A-3. After simplifying, eqs A-3 can be rewritten as

$$-\ln\left(\frac{\mathscr{R}_{2k-1}}{\langle|\omega|^{2k-1}\rangle_0}\right) \cong \begin{cases} \dfrac{\langle\omega^{2k-1}\rangle}{\langle|\omega|^{2k-1}\rangle_0} & \text{if } \langle\omega^{2k-1}\rangle \geq 0 \\ -\dfrac{\langle\omega^{2k-1}\rangle}{\langle|\omega|^{2k-1}\rangle_0} & \text{if } \langle\omega^{2k-1}\rangle < 0 \end{cases} \qquad \text{(A-6)}$$

Finally, eq A-6 can be rearranged and condensed to obtain eq 8:

$$\frac{\langle|\omega|^{2k-1}\rangle}{\langle|\omega|^{2k-1}\rangle_0} \cong \frac{|\langle\omega^{2k-1}\rangle|}{\langle|\omega|^{2k-1}\rangle_0} + \exp\left(-\frac{|\langle\omega^{2k-1}\rangle|}{\langle|\omega|^{2k-1}\rangle_0}\right) \qquad (8)$$

References and Notes

(1) Rubinstein, M.; Colby, R. H. *Polymer Physics*; Oxford University Press: New York, 2003.
(2) Flory, P. J. *Principles of Polymer Chemistry*; Cornell University Press: Ithaca, NY, 1953.
(3) Mark, J. E.; Erman, B. *Rubberlike Elasticity: A Molecular Primer*; Wiley: New York, 1988; p 196.
(4) Mark, J. E. *Prog. Polym. Sci.* **2003**, *28*, 1205–1221.
(5) Deloche, B.; Samulski, E. T. *Macromolecules* **1981**, *14*, 575–581.
(6) Deloche, B.; Dubault, A.; Herz, J.; Lapp, A. *EPL* (*Europhys. Lett.*) **1986**, *1*, 629–635.
(7) Sotta, P.; Deloche, B.; Herz, J.; Lapp, A.; Durand, D.; Rabadeux, J. C. *Macromolecules* **1987**, *20*, 2769–2774.
(8) Sotta, P.; Deloche, B. *Macromolecules* **1990**, *23*, 1999–2007.
(9) Kornfield, J. A.; Chung, G. C.; Smith, S. D. *Macromolecules* **1992**, *25*, 4442–4444.
(10) Sotta, P. *Macromolecules* **1998**, *31*, 3872–3879.
(11) Hedden, R. C.; McCaskey, E.; Cohen, C.; Duncan, T. M. *Macromolecules* **2001**, *34*, 3285–3293.
(12) Hedden, R. C.; Tachibana, H.; Duncan, T. M.; Cohen, C. *Macromolecules* **2001**, *34*, 5540–5546.
(13) Callaghan, P. T.; Samulski, E. T. *Macromolecules* **2003**, *36*, 724–735.
(14) Batra, A.; Hedden, R. C.; Schofield, P.; Barnes, A.; Cohen, C.; Duncan, T. M. *Macromolecules* **2003**, *36*, 9458–9466.
(15) Chapellier, B.; Deloche, B.; Oeser, R. *J. Phys. II* **1993**, *3*, 1619–1631.
(16) Depner, M.; Deloche, B.; Sotta, P. *Macromolecules* **1994**, *27*, 5192–5199.
(17) Sotta, P.; Higgs, P. G.; Depner, M.; Deloche, B. *Macromolecules* **1995**, *28*, 7208–7214.
(18) Jacobi, M. M.; Abetz, V.; Stadler, R.; Gronski, W. *Polymer* **1996**, *37*, 1669–1675.
(19) Ries, M. E.; Brereton, M. G.; Klein, P. G.; Ward, I. M.; Ekanayake, P.; Menge, H.; Schneider, H. *Macromolecules* **1999**, *32*, 4961–4968.
(20) Edwards, S. F.; McLeish, T. C. B. *J. Chem. Phys.* **1990**, *92*, 6855–6857.
(21) Brereton, M. G. *Macromolecules* **1993**, *26*, 1152–1157.
(22) Yong, C. W.; Higgs, P. G. *Macromolecules* **1999**, *32*, 5062–5071.
(23) Saalwächter, K.; Ziegler, P.; Spyckerelle, O.; Haidar, B.; Vidal, A.; Sommer, J. *J. Chem. Phys.* **2003**, *119*, 3468–3482.
(24) Genesky, G. D.; Aguilera-Mercado, B. M.; Bhawe, D. M.; Escobedo, F. A.; Cohen, C. *Macromolecules* **2008**, *41*, 8231–8241.
(25) Genesky, G. D.; Duncan, T. M.; Cohen, C. *Macromolecules* **2009**, DOI: 10.1021/ma901712s.
(26) Saalwächter, K.; Kleinschmidt, F.; Sommer, J. *Macromolecules* **2004**, *37*, 8556–8568.
(27) Saalwächter, K.; Sommer, J. *Macromol. Rapid Commun.* **2007**, *28*, 1455–1465.
(28) Saalwächter, K. *Prog. Nucl. Magn. Reson. Spectrosc.* **2007**, *51*, 1–35.
(29) Gjersing, E.; Chinn, S.; Giuliani, J. R.; Herberg, J.; Maxwell, R. S.; Eastwood, E.; Bowen, D.; Stephens, T. *Macromolecules* **2007**, *40*, 4953–4962.
(30) Weese, J. *Comput. Phys. Commun.* **1992**, *69*, 99–111.
(31) Tikhonov, A. N.; Arsenin, V. Y. *Solutions of Ill-Posed Problems*; Winston: WA, 1977; p 258.
(32) Schäfer, H.; Stannarius, R. *J. Magn. Res., Ser. B* **1995**, *106*, 14–23.
(33) Winterhalter, J.; Maier, D.; Grabowski, D. A.; Honerkamp, J.; Muller, S.; Schmidt, C. *J. Chem. Phys.* **1999**, *110*, 4035–4046.
(34) Schäfer, H.; Mädler, B.; Sternin, E. *Biophys. J.* **1998**, *74*, 1007–1014.
(35) van Beek, J. D.; Meier, B. H.; Schäfer, H. *J. Magn. Reson.* **2003**, *162*, 141–157.
(36) Wendlandt, M.; van Beek, J. D.; Suter, U. W.; Meier, B. H. *Macromolecules* **2005**, *38*, 8372–8380.
(37) Jaynes, E. T. *Phys. Rev.* **1957**, *106*, 620.
(38) Jaynes, E. T. *Phys. Rev.* **1957**, *108*, 171.
(39) Jaynes, E. T. *Probability Theory: The Logic of Science*; Bretthorst, G. L., Ed.; Cambridge University Press: Cambridge, U.K., 2003; p 727.
(40) Brown, W.; Johnsen, R.; Stepanek, P.; Jakes, J. *Macromolecules* **1988**, *21*, 2859–2865.
(41) Runge, A. F.; Saavedra, S. S.; Mendes, S. B. *J. Phys. Chem. B* **2006**, *110*, 6721–6731.
(42) Berardi, R.; Spinozzi, F.; Zannoni, C. *J. Chem. Phys.* **1998**, *109*, 3742–3759.
(43) Sakakibara, D.; Sasaki, A.; Ikeya, T.; Hamatsu, J.; Hanashima, T.; Mishima, M.; Yoshimasu, M.; Hayashi, N.; Mikawa, T.; Walchli, M.; Smith, B. O.; Shirakawa, M.; Guntert, P.; Ito, Y. *Nature* **2009**, *458*, 102–105.
(44) Thaning, J.; Stevensson, B.; Östervall, J.; Naidoo, K. J.; Widmalm, G.; Maliniak, A. *J. Phys. Chem. B* **2008**, *112*, 8434–8436.
(45) Chiang, Y.; Borbat, P. P.; Freed, J. H. *J. Magn. Reson.* **2005**, *177*, 184–196.
(46) Genesky, G. D.; Aguilera-Mercado, B. M.; Escobedo, F. A.; Cohen, C. *Macromolecules* **2009**; manuscript in preparation).
(47) Cohen-Addad, J. P. *J. Chem. Phys.* **1974**, *60*, 2440–2453.
(48) Cohen-Addad, J. P.; Domard, M.; Herz, J. *J. Chem. Phys.* **1982**, *76*, 2744–2753.
(49) Carmesin, I.; Kremer, K. *Macromolecules* **1988**, *21*, 2819.
(50) Binder, K.; Paul, W. *J. Polym. Sci., Polym. Phys.* **1997**, *35*, 1.
(51) Paul, W.; Binder, K.; Heermann, D.; Kremer, K. *J. Phys. II* **1991**, *1*, 37.
(52) Escobedo, F. A.; de Pablo, J. J. *J. Chem. Phys.* **1997**, *106*, 793–810.
(53) Chen, Z.; Cohen, C.; Escobedo, F. A. *Macromolecules* **2002**, *35*, 3296–3305.
(54) Bhawe, D. M.; Cohen, C.; Escobedo, F. A. *Macromolecules* **2004**, *37*, 3924–3933.